№ 216/200 – BIV – 18/11/20 – Число полос: 6

https://doi.org/10.1070/QEL00000

Production of two-colour radiation with polarisations of components rotating in opposite directions

V.M. Kotov

Abstract. **A method is proposed for the production of two-colour radiation with monochromatic components, the polarisation vectors of which rotate in opposite directions, and the rotation speed is controlled by the sound frequency. The method is based on acousto-optic (AO) interaction upon double passage of two-colour radiation through an AO cell made of a gyrotropic crystal; the method efficiency is demonstrated by the example of radiation from an Ar laser generating at wavelengths of 0.488 and 0.514 μm and an AO cell made of TeO_2, operating at a sound frequency of 60 MHz.**

Keywords: *two-colour optical radiation, acousto-optic diffraction, Bragg regime, rotation of the polarisation vector.*

1. Introduction

Acousto-optic (AO) diffraction is widely used to control the parameters of optical radiation – its amplitude, frequency, phase, polarisation, etc. [1 – 3]. It allows one to generate an optical beam with the 'desired' characteristics, for example, to rotate the polarisation vector with a frequency controlled by the sound frequency (see, for example, [4 – 7]). The authors of Refs [8 – 10] experimentally obtained the polarisation rotation frequencies equal to two and four times the frequency of sound. Radiation with a rotating polarisation vector makes it possible to ensure high-frequency amplitude modulation of an optical beam, while the modulation frequency can be several times higher than the pulse modulation frequency [11]; polarisation rotation finds application in Doppler anemometry systems [12], etc.

In all the mentioned works, only monochromatic radiation was used. In this paper, we propose a method for the production of two-colour radiation with rotating vectors of polarisations of monochromatic components, the polarisations rotating in opposite directions. The frequency of rotation of both components, as will be shown below, is equal to the frequency of sound. This radiation can be used, for example, to analyse the dispersion properties of liquid crystals [13, 14], to study crystals under the influence of electric fields [15], to examine the properties of complex molecular compounds (see, for example, [16]), and to find application in pharmaceuticals (for analysis of variance of optically active drugs, sugars [17], etc.). The proposed method can be used as the basis for the development of a whole class of devices, i. e. two-colour polarimeters designed to measure the polarisation characteristics of transparent media simultaneously at two wavelengths. This significantly expands the possibilities of using AO diffraction for solving various applied problems.

V.M. Kotov Kotel'nikov Institute of Radioengineering and Electronics (Fryazino Branch), Russian Academy of Sciences, pl. Vvedenskogo 1, 141190 Fryazino, Moscow region, Russia;
e-mail: vmk277@ire216.msk.su

Received 6 August 2020
Kvantovaya Elektronika **50** (12) 1167 – 1172 (2020)
Translated by I.A. Ulitkin

2. Theory

The production of two-colour radiation with polarisation vectors rotating in opposite directions is explained using two vector diagrams (Fig. 1). The first diagram (Fig. 1a) displays the process of AO interaction when light propagates through the AO cell in the forward direction; the second one (Fig. 1b), in the opposite direction, after the light is reflected from the prism. We assume that the AO medium is a uniaxial gyrotropic paratellurite (TeO_2) crystal. Two-colour optical radiation $\boldsymbol{T}$ with wavelengths λ_1 and λ_2 is incident on the (001) face of the TeO_2 crystal at an angle α to its optical axis [001]. Inside the crystal, radiation decays into monochromatic components with wavelengths λ_1 and λ_2, each of which is split into two eigenwaves. Figure 1 shows only those eigenwaves that participate in AO diffraction. The selected waves belong to the 'inner' surfaces of the wave vectors ('fast' eigenwaves). As a result of the anisotropic AO interaction, they diffract into 'slow' waves belonging to 'outer' wave surfaces. Other eigenwaves of incident radiation are not shown in the figure in order not to overload it. However, they play an important role in the formation of the final optical radiation, and so their presence is always assumed. An acoustic wave with a wave vector $\boldsymbol{q}$ propagates along the [110] axis. The wave vectors of the incident waves with wavelengths λ_1 and λ_2 are designated by $\boldsymbol{K}_{1\mathrm{i}}$ and $\boldsymbol{K}_{2\mathrm{i}}$; the waves are diffracted in the directions $\boldsymbol{K}_{1\mathrm{d}}$ and $\boldsymbol{K}_{2\mathrm{d}}$, respectively. At the output from the crystal, all beams are reflected from the prism Pr with an apex angle of 90° and propagate through the AO cell in strictly opposite directions (see Fig. 1 b). Note that since the beams are reflected twice from the surfaces of the prism, the polarisations of the reflected beams coincide with those of the beams incident on the prism. This point is especially important when using TeO_2, since its eigenwaves are generally elliptically polarised. Waves $\boldsymbol{K}_{1\mathrm{i}}$, $\boldsymbol{K}_{2\mathrm{i}}$, $\boldsymbol{K}_{1\mathrm{d}}$ and $\boldsymbol{K}_{2\mathrm{d}}$ in the first diagram transform into waves $\boldsymbol{K}_{1\mathrm{i}}$, $\boldsymbol{K}_{2\mathrm{i}}$, $\boldsymbol{K}_{1\mathrm{d}}$ and $\boldsymbol{K}_{2\mathrm{d}}$ in the second diagram. Waves $\boldsymbol{K}_{1\mathrm{i}}$ and $\boldsymbol{K}_{2\mathrm{i}}$ at 100 % diffraction efficiency are completely diffracted into waves $\boldsymbol{K}_{1\mathrm{d}}$ and $\boldsymbol{K}_{2\mathrm{d}}$, which, being transformed into $\tilde{\boldsymbol{K}}_{1\mathrm{d}}$ and $\tilde{\boldsymbol{K}}_{2\mathrm{d}}$, return to waves $\tilde{\boldsymbol{K}}_{1\mathrm{i}}$ and $\tilde{\boldsymbol{K}}_{2\mathrm{i}}$. However, the frequencies of the waves $\tilde{\boldsymbol{K}}_{1\mathrm{i}}$ and $\tilde{\boldsymbol{K}}_{2\mathrm{i}}$ emerging from the AO cell after double passage will differ from the frequencies of the original waves $\boldsymbol{K}_{1\mathrm{i}}$ and $\boldsymbol{K}_{2\mathrm{i}}$. Indeed, as follows from the vector diagrams, the wave $\boldsymbol{K}_{1\mathrm{d}}$ is formed as a result

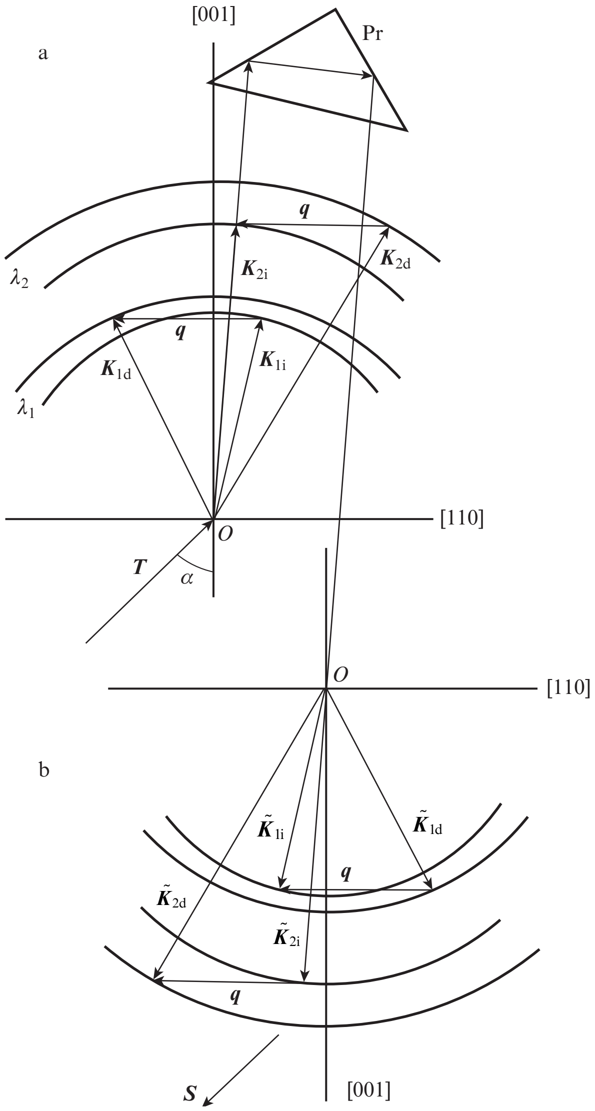

Figure 1. Vector diagram of the AO diffraction of two-colour radiation when light propagates through the AO cell in (a) the forward and (b) backward directions.

of the reflection of the wave $\boldsymbol{K}_{1i}$ from the 'incoming' acoustic wave $\boldsymbol{q}$; therefore, due to the Doppler effect, the frequency of the wave $\boldsymbol{K}_{1d}$ is $\omega_1 + \Omega$ (here ω_1 and Ω are the cyclic frequencies of the wave $\boldsymbol{K}_{1i}$ and the sound wave, respectively). Another diffracted wave $\boldsymbol{K}_{2d}$ is produced as a result of the reflection of $\boldsymbol{K}_{2i}$ from the 'outgoing' sound wave $\boldsymbol{q}$, and its frequency is equal to $\omega_2 - \Omega$, where ω_2 is the cyclic frequency of the wave $\boldsymbol{K}_{2i}$. After reflection from the prism Pr and re-passing through the AO cell, the wave $\tilde{\boldsymbol{K}}_{1d}$ (with the frequency $\omega_1 + \Omega$) is reflected from the 'incoming' sound wave $\boldsymbol{q}$, and so the frequency of the wave $\tilde{\boldsymbol{K}}_{1i}$ will be equal to $\omega_1 + 2\Omega$. Similarly, we obtain that the wave $\tilde{\boldsymbol{K}}_{2i}$ has the frequency $\omega_2 - 2\Omega$. Thus, at the output of the AO cell, two waves $\tilde{\boldsymbol{K}}_{1i}$ and $\tilde{\boldsymbol{K}}_2$ are produced with frequencies $\omega_1 + 2\Omega$ and $\omega_2 - 2\Omega$; they 'merge' with each other, as well as with other eigenwaves that do not participate in diffraction, into the outgoing two-colour radiation $\boldsymbol{S}$.

Next, we will determine the frequency-angular characteristics of diffraction when two optical waves interact with one acoustic wave. Note that a similar problem has already been solved in [18] using the surfaces of wave vectors of a uniaxial gyrotropic crystal described by fourth-order equations. The solutions were obtained only numerically. In the present work, a simplified model is used, which, however, allows obtaining analytical expressions with an error of no more than 1%–2% from exact computer solutions. We will describe the surfaces of wave vectors of a uniaxial gyrotropic crystal in the form [7, 19]

$$\frac{K_x^2}{K_e^2} + \frac{K_z^2}{K_o^2}(1 + n_o^2 g_{33}) = 1,$$
$$\frac{K_x^2}{K_e^2} + \frac{K_z^2}{K_o^2}(1 - n_o^2 g_{33}) = 1, \qquad (1)$$

where K_x and K_z are the projections of the wave vector of light on [110] and [001] axes, respectively; $K_o = 2\pi n_o \lambda^{-1}$; $K_e = 2\pi n_e \lambda^{-1}$; n_o and n_e are the main refractive indices of a uniaxial crystal; g_{33} is the component of the gyration pseudotensor [20]; and λ is the wavelength of light. The first equation in (1) describes the 'inner' surface of the wave vectors; the second one, the 'outer' surface under the assumption that the crystal is positive uniaxial ($n_e > n_o$).

The course of solving the problem, which makes it possible to simply obtain the necessary expressions, is explained using a vector diagram (Fig. 2), which shows the wave surfaces of a uniaxial gyrotropic crystal for radiation with wavelengths λ_1 and λ_2. At the first stage, we assume that the incident two-colour radiation propagates strictly along the optical axis [001]. The acoustic wave is directed along the [110] axis. Two-colour radiation is represented by wave vectors $\boldsymbol{K}_1$ and $\boldsymbol{K}_2$, which belong to the 'inner' wave surfaces. As a result of anisotropic diffraction, the beam $\boldsymbol{K}_1$ is diffracted by the acoustic wave $\boldsymbol{q}_1$ in the $\boldsymbol{K}_{1d}$ direction, and the beam $\boldsymbol{K}_2$ is diffracted by the wave $\boldsymbol{q}_2$ in the $\boldsymbol{K}_{2d}$ direction. In general, $\boldsymbol{q}_1$ and $\boldsymbol{q}_2$ are not equal to each other. To find the value of $\boldsymbol{q}_1$, we set $K_x = 0$ in equations (1). Then we have

$$K_{z1} = \frac{K_o}{\sqrt{1 + n_o^2 g_{33}}} \qquad (2)$$

for the 'inner' surface and

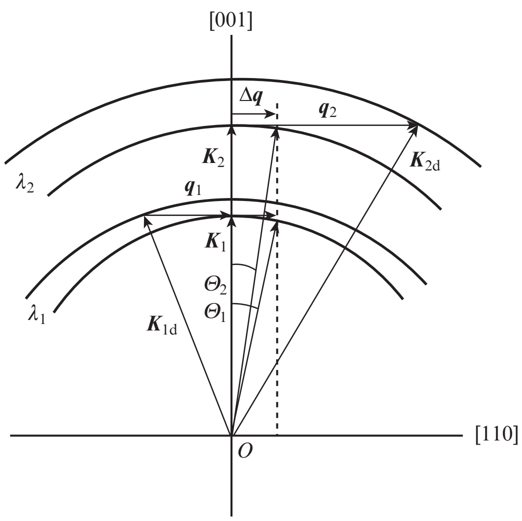

Figure 2. Vector diagram for calculating the frequency and angular characteristics of diffraction.

$$K_{z2} = \frac{K_o}{\sqrt{1 - n_o^2 g_{33}}} \tag{3}$$

for the 'outer' surface. Since in our case there is anisotropic diffraction, in which the wave vector belonging to the 'inner' surface diffracts in the direction of the vector belonging to the 'outer' surface, we substitute the expression for K_{z1} (2) into the second equation of system (1). As a result, we obtain that K_x is equal to the modulus of the sound vector $\boldsymbol{q}_1$:

$$K_x = q_1 = \frac{2\pi}{\lambda_1} n_e \sqrt{\frac{2n_o^2 g_{33}}{1 + n_o^2 g_{33}}}. \tag{4}$$

Similarly, we determine the value of $\boldsymbol{q}_2$:

$$q_2 = \frac{2\pi}{\lambda_2} N_e \sqrt{\frac{2N_o^2 G_{33}}{1 + N_o^2 G_{33}}}. \tag{5}$$

In expressions (4) and (5), the parameters n_o, n_e, and g_{33} refer to radiation with wavelength λ_1, and N_o, N_e, and G_{33} refer to radiation with λ_2. Simultaneous diffraction of radiation with wavelengths λ_1 and λ_2 is possible only when the values of the wave vectors of sound coincide. To 'align' the wave vectors $\boldsymbol{q}_1$ and $\boldsymbol{q}_2$, we add some vector $\Delta\boldsymbol{q}$ to $\boldsymbol{q}_1$ and subtract the same vector $\Delta\boldsymbol{q}$ from the vector $\boldsymbol{q}_2$. Then diffraction will occur on sound, the wave vector of which takes the form

$$\boldsymbol{Q} = \boldsymbol{q}_1 + \Delta\boldsymbol{q} = \boldsymbol{q}_2 - \Delta\boldsymbol{q}, \tag{6}$$

therefore,

$$\boldsymbol{Q} = (\boldsymbol{q}_1 + \boldsymbol{q}_2)/2, \tag{7}$$

$$\Delta\boldsymbol{q} = (\boldsymbol{q}_2 - \boldsymbol{q}_1)/2. \tag{8}$$

Using the relation $Q = 2\pi f/V$, where f and V are the frequency and speed of sound, as well as expressions (4), (5) and (7), we find the frequency f

$$f = \frac{V}{2}\left[\frac{n_e}{\lambda_1}\sqrt{\frac{2n_o^2 g_{33}}{1 + n_o^2 g_{33}}} + \frac{N_e}{\lambda_2}\sqrt{\frac{2N_o^2 G_{33}}{1 + N_o^2 G_{33}}}\right]. \tag{9}$$

The displacement of the vectors of sound, $\boldsymbol{q}_1$ and $\boldsymbol{q}_2$ by $\Delta\boldsymbol{q}$, generally speaking, leads to the fact that the waves $\boldsymbol{K}_1$ and $\boldsymbol{K}_2$ will propagate not along the optical axis, but at angles Θ_1 and Θ_2 to it. These angles, strictly speaking, are the angles of refraction of two-colour radiation at the input face (001), with the angle Θ_1 being greater than Θ_2. With a good approximation, we can set $\Theta_1 = \Delta q/K_{z1}$ and consider this angle as the maximum angle Θ_{max} of the deviation of the beams $\boldsymbol{K}_1$ and $\boldsymbol{K}_2$ from the [001] axis. Taking into account relations (4), (5) and (8), we have

$$\Theta_{max} \approx \frac{\sqrt{1 + n_o^2 g_{33}}}{2n_o}\left(\frac{\lambda_1}{\lambda_2} N_e \sqrt{\frac{2N_o^2 G_{33}}{1 + N_o^2 G_{33}}} - n_e \sqrt{\frac{2n_o^2 g_{33}}{1 + n_o^2 g_{33}}}\right). \tag{10}$$

The angle Θ_{max} determines the ellipticity ρ of the wave, farthest from the optical axis [21]:

$$\rho = \frac{1}{g_{33}}\left[\sqrt{\tan^4\Theta_{max}\left(\frac{1}{n_o^2} - \frac{1}{n_e^2}\right)^2 + 4g_{33}^2} - \tan^2\Theta_{max}\left(\frac{1}{n_o^2} - \frac{1}{n_e^2}\right)\right]. \tag{11}$$

To obtain specific values of the quantities determined by expressions (9), (10) and (11), we will assume that two-colour radiation is generated by an Ar laser. The radiation is diffracted by an acoustic wave propagating in TeO_2. Based on the data from [22, 23], we have

$$\lambda_1 = 0.5145 \times 10^{-4}\ \text{cm}, \quad n_o = 2.3115, \quad n_e = 2.4735,$$

$$g_{33} = 3.69 \times 10^{-5};$$

$$\lambda_2 = 0.488 \times 10^{-4}\ \text{cm}, \quad N_o = 2.3303, \quad N_e = 2.494,$$

$$G_{33} = 3.93 \times 10^{-5}, \quad V = 0.617 \times 10^5\ \text{cm s}^{-1}.$$

After substitution, we obtain $f \approx 62$ MHz, $\Theta_{max} \approx 0.06°$, and $\rho = 0.99$. It is seen that the value of ρ is close to unity, i. e. the eigenwaves of the crystal that produce two-colour radiation have virtually circular polarisations. Note that for the same wavelengths of optical radiation, $f = 60$ MHz and $\Theta = 0.062°$ were obtained in [18]. Thus, the values obtained using expressions (9), (10) and (11) differ from the corresponding values in [18] by no more than 1%–2%.

Let us consider the result of the combining of the waves at the crystal output. We assume for definiteness that the polarisations of the waves $\boldsymbol{K}_{1i}$ and $\boldsymbol{K}_{2i}$ belonging to the 'inner' surfaces of the wave vectors (see Fig. 1) are left-hand circular, and the polarisations of the waves $\boldsymbol{K}_{1d}$ and $\boldsymbol{K}_{2d}$ are right-hand circular. Then the outgoing waves $\tilde{\boldsymbol{K}}_{1i}$ and $\tilde{\boldsymbol{K}}_{2i}$ will be left-hand circular; they are combined at the output with right-hand circular waves that do not participate in diffraction. The total beam with wavelength λ_1 is produced as a result of the combining of a left-hand circular wave with frequency $\omega_1 + 2\Omega$ and a right-hand circular wave with frequency ω_1. Similarly, the total beam with the wavelength λ_2 is produced as a result of the combining of the left-hand circular wave with frequency $\omega_2 - 2\Omega$ and the right-hand circular wave with frequency ω_2.

Let us further consider the combining of the eigenwaves that make up the radiation with the wavelength λ_1. By assuming that radiation propagates along a certain direction OZ and the amplitudes of all the waves are equal to each other and to unity, the projections of the electric vector e_{x1} and e_{y1} onto the directions OX and OY, orthogonal to OZ, for radiation with right-hand circular polarisation, which does not participate in diffraction, can be written in the form

$$e_{x1} = \cos(\omega_1 t); \quad e_{y1} = \sin(\omega_1 t), \tag{12}$$

and the projections e_{x2} and e_{y2} for radiation with left-hand circular polarisation, twice participating in diffraction, can be written in the form

$$e_{x2} = \cos[(\omega_1 + 2\Omega)t]; \quad e_{y2} = -\sin[(\omega_1 + 2\Omega)t]. \tag{13}$$

We write the total fields along OX and OY as $e_x = e_{x1} + e_{x2}$ and $e_y = e_{y1} + e_{y2}$. After simple transformations we obtain

$$e_x = 2\cos(\Omega t)\cos[(\omega_1 + 2\Omega)t],$$
$$e_y = -2\sin(\Omega t)\cos[(\omega_1 + 2\Omega)t]. \tag{14}$$

The fast-variable component of both signals $\cos[(\omega_1 + 2\Omega)t]$ changes, in fact, with frequency ω_1, because $\omega_1 \gg \Omega$. The photodetector does not have time to track this component and averages it. Since the photodetector operates in a quadratic regime, it 'averages' the function $\cos^2(2\omega_1)$, the average value of which is 1/2. For signal amplitudes (14), we introduce the notation

$$\alpha_x = \cos(\Omega t), \quad \alpha_y = -\sin(\Omega t). \tag{15}$$

It can be seen that the nature of the change in the amplitudes α_x and α_y is similar to the change in functions (13), i.e. α_x and α_y demonstrate left-hand circular rotation of the polarisation vector with frequency Ω. This frequency falls within the range of frequencies measured by the photodetector, and therefore it is easily tracked in the experiment.

A similar procedure can be performed with radiation λ_2. In this case, the signal amplitudes have the form

$$A_x = \cos(\Omega t), \quad A_y = \sin(\Omega t), \tag{16}$$

i.e. right-hand circular rotation of polarisation with frequency Ω.

Thus, it can be argued that as a result of the combining, circularly polarised eigenwaves with different frequencies produce radiation with linear slowly rotating polarisation, while the direction of rotation of the polarisation vector is determined by the ratio between the frequencies of the combined waves. For example, if, as a result of the AO interaction, the frequency of the 'fast' eigenwave decreases relative to the frequency of the 'slow' wave, then when the waves are combined, the rotation of the polarisation vector will be in one direction, and if the frequency increases, the rotation is reversed.

3. Experiment and discussion of the results

An experimental setup for observing the effect of polarisation rotation in opposite directions is shown in Fig. 3. Two-colour radiation generated by the laser passes through an attenuator A and a $\lambda/4$ plate; then it is directed to the AOM cell, passes through it, and returns to the cell after reflection from a prism Pr. The prism performs several functions: it reflects the beams in directions collinear with the beams incident on the prism, ensures the separation of beams passing through the AO cell in the forward and reverse directions, and also preserves the polarisation of the beams after they are reflected from the prism. The radiation transmitted in the opposite direction through the AO cell is incident on a mirror M; after being reflected from it, it passes a polariser P and is incident on a photodetector PD. The signal from the photodetector is fed to an oscilloscope. A generator is the source of sinusoidal signals that control the AO cell and provides synchronisation of the oscilloscope. The source of two-colour radiation is an Ar laser, which generates two brightest, linearly polarised lines with wavelengths of 0.514 and 0.488 μm. The AO cell is made of a TeO_2 single crystal measuring $1.0 \times 0.8 \times 1.0$ cm along the [110], [110], and [001] directions, respectively. A $LiNbO_3$ transducer is glued to the (110) face of the crystal, generating a transverse acoustic wave with a shear direction along [110]. The speed of sound in the crystal is 617 m s_{-1}. The length of the AO interaction is 0.6 cm; the sound frequency is 60 ± 2 MHz at a 3-dB level.

The experiment consisted of two stages. The first stage involved the tuning of the AO cell to obtain the best conditions for the diffraction of two-colour radiation. To this end, instead of the prism Pr, a screen was installed behind the AO cell. The screen was used to ensure the angular adjustment of the cell, as well as the adjustment of the frequency and sound power. In this case, the propagation of diffracted beams on different sides of the incident radiation was controlled. After adjusting the AO cell, the second stage of the experiment was performed, i.e. instead of the screen, the prism Pr was installed, which was located almost close to the AO cell. Then a mirror M was adjusted, and the photodetector PD was also adjusted to obtain the maximum electrical signal. In this case, the photodetector was tuned only to the zero Bragg order, since, as follows from Fig. 1, it registers both the waves that do not participate in diffraction and the waves that have diffracted twice on an acoustic wave. In the experiments, only one photodetector was used, which separately measured the characteristics of the monochromatic components of the laser radiation. For this purpose, IF interference filters were installed at the output of the laser after the attenuator, transmitting radiation either with a wavelength of λ_1 or λ_2. Figure 4 shows a photograph of the signal fed from the photodetector to the frequency counter. Measurements showed that the waveforms of both monochromatic components are the same and coincide with the waveform of the generator. This fact is

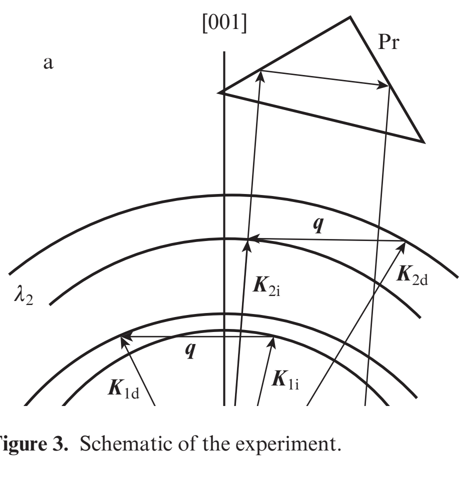

Figure 3. Schematic of the experiment.

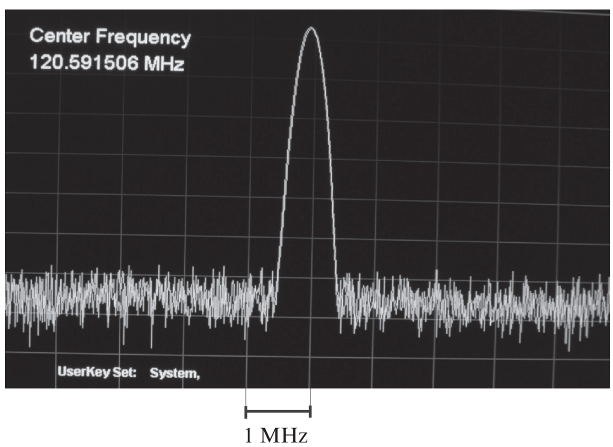

Figure 4. Typical monochromatic frequency signal on a frequency counter. The scale division is 1 MHz.

fundamentally important for a number of optoelectronic devices, for example, for anemometers [24, 25].

The rotation of the polarisation vector of the monochromatic components was checked by rotating the polariser P installed in front of the photodetector PD. Figure 5 shows the signals from laser radiation with λ_1 [curve (*1*)] and λ_2 [curve (*2*)], obtained alternately on the oscilloscope screen. The signal levels are different, since the intensity of the line with λ_1 = 0.514 μm is almost twice the intensity of the line with λ_2 = 0.488 μm. Figure 5 also displays the signal from the generator [curve (*3*)], the frequency of which coincides with the frequency fed to the AO cell, and is half the frequency of signals *1* and *2*. This is due to the fact that, although the photodetector PD receives a light signal modulated at the sound frequency Ω [see expressions (15) and (16)], the photodetector operates in a quadratic regime, and therefore it registers a signal at a doubled frequency of 2Ω. The modulation depth of signals *1* and *2* was ~15%. Such a low depth can be caused by several factors: it was not possible to ensure 100% diffraction efficiency; beams propagating through the AO cell in forward and backward directions interact with different efficiency; there is diffraction and other diffraction orders, which reduces the amplitude of the waves that are twice diffracted on the sound wave; complete coincidence of the interfering fields at the exit of light from the cell is not achieved; inhomogeneities of the crystal, optical and acoustic fields, etc., can also be of importance. Nevertheless, clear sinusoidal signals have been obtained, which make it possible to reliably measure their frequency, amplitude, and phase characteristics.

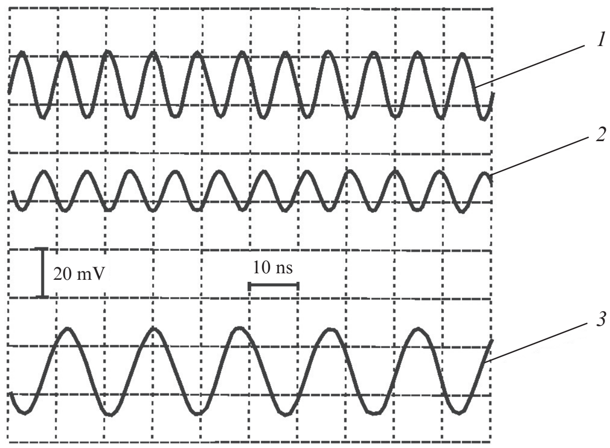

Figure 5. Signals demonstrating the rotation of polarisations of monochromatic components with wavelengths of (*1*) 0.514 and (*2*) 0.488 μm, as well as (*3*) a signal coming from a generator. The oscilloscope time base division is 10 ns.

When the polariser is rotated, signals *1* and *2* are displaced in opposite directions, while their amplitudes do not change. This indicates the presence of rotation of the polarisation vectors of optical beams in opposite directions. The displacement of the signals by 360° corresponds to rotation of the polarizer by 180°. In our experiments, the signal displacement was symmetrical. If an optically active medium (for example, a sugar solution) is placed after the polariser and its concentration is changed, then an asymmetric shift of signals from two different wavelengths can be observed. The latter can be used to measure the dispersion of optical rotation; however, measurements of optically active media were not the purpose of this work and will be the subject of separate studies.

4. Conclusions

To produce two-colour optical radiation, the polarisations of the monochromatic components of which rotate in opposite directions, we used AO diffraction regimes where one of the components diffracts with decreasing frequency (to the frequency of sound), and the other diffracts with increasing frequency. The AO medium is a gyrotropic crystal, whose eigenwaves are circularly polarised.

A scheme of AO diffraction is proposed, based on two acts of AO interaction of each monochromatic component. According to the scheme, the frequencies of the diffracted beams with wavelengths λ_1 and λ_2 return to the frequencies ω_1 and ω_2 of the fundamental radiation, and the frequencies of the returning beams become equal to $\omega_1 + 2\Omega$ and $\omega - 2\Omega$, where Ω is the sound frequency.

The method is demonstrated by the example of two-colour radiation of an Ar laser with lasing lines at 0.514 and 0.488 μm. A uniaxial gyrotropic TeO_2 crystal, in which a transverse acoustic wave with a frequency of ~ 60 MHz was excited, was chosen as an AO medium. The rotation of the polarisation vectors of the monochromatic components in opposite directions is confirmed by rotating the linear polariser located in front of the photodetector.

The results obtained can find application for the development of devices using two-colour radiation with rotating polarisation vectors, the speed and direction of rotation of light in which are controlled by an acoustic wave.

Acknowledgements. The work was performed as part of the State Assignment (Topic 0030-2019-0014) and partially supported by the Russian Foundation for Basic Research (Grant No. 19-07-00071).

References

1. Magdich L.N., Molchanov V.Ya. *Acousto-Optical Devices and Their Application* (New York: Gordon and Breach, 1989; Moscow: Sov. Radio, 1978).
2. Balakshy V.I., Parygin V.N., Chirkov L.E. *Fizicheskie printsypy akustooptiki* (Physical Principles of Acoustooptics) (Moscow: Radio i Svyaz', 1985).
3. Xu J., Stroud R. *Acousto-Optic Devices: Principles, Design, and Applications* (New York: John Wiley & Sons Inc., 1992).
4. Shamir J., Fainman Y. *Appl. Opt.*, **21** (3), 364 (1982).
5. Kotov V.M., Averin S.V., Kotov E.V., Voronko A.I., Tikhomirov S.A. *Quantum Electron.*, **47** (2), 135 (2017) [*Kvantovaya Elektron.*, **47** (2), 135 (2017)].
6. Kotov V.M., Kotov E.V. *Opt. Zh.*, **84** (6), 51 (2017).
7. Kotov V.M., Kotov E.V. *Quantum Electron.*, **48** (8), 773 (2018) [*Kvantovaya Elektron.*, **48** (8), 773 (2018)].
8. Kotov V.M., Averin S.V., Kotov E.V. *Opt. Zh.*, **86** (3), 3 (2019).
9. Kotov V.M., Averin S.V., Shkerdin G.N. *Quantum Electron.*, **46** (2), 179 (2016) [*Kvantovaya Elektron.*, **46** (2), 179 (2016)].
10. Kotov V.M., Averin S.V., Kotov E.V. *Prikl. Fiz.*, (3), 65 (2016).
11. Kotov V.M., Averin S.V., Shkerdin G.N. *Radiotekh. Elektron.*, **64** (10), 138 (2019).
12. Kotov V.M., Voronko A.I., Tikhomirov S.A. *Prib. Tekh. Eksp.*, (4), 89 (2019).
13. Konshina E.A., Fedorov M.A., Amosova L.P. *Opt. Zh.*, **73** (12), 9 (2006).
14. Konshina E.A., Kostomarov D.S. *Opt. Zh.*, **74** (10), 88 (2007).
15. Vasil'ev A.A., Kasasent D., Kompanets I.N., Parfenov A.V. *Prostranstvennye modulyatory sveta* (Spatial Light Modulators) (Moscow: Radio i svyaz', 1987).

16. Kolbina G.F., Grishchenko A.E., Sazanov Yu.N., Shtennikova I.N. *Vysokomolek. Soed., Ser. A*, **51** (7), 1104 (2009).
17. Ramenskoi G.V. (Ed.) *Farmatsevticheskaya khimiya: uchebnik* (A Texbook of Pharmaceutical Chemistry) (Moscow: BINOM, 2015).
18. Kotov V.M. *Opt. Spektrosk.*, **77** (3), 493 (1994).
19. Chernyatin A.Yu. *Cand. Dis.* (Moscow, Lomonosov Moscow State University, 2003).
20. Sirotin Yu.I., Shaskol'skaya M.P. *Osnovy kristallofiziki* (Fundamentals of Crystal Physics) (Moscow: Nauka, 1979).
21. Yariv A., Yukh P. *Optical Waves in Crystals: Propagation and Control of Laser Radiation* (New York: Wiley, 2003; Moscow: Mir, 1987).
22. Shaskol'skaya M.P. (Ed.) *Akusticheskie kristally* (Acoustic Crystals) (Moscow: Nauka, 1982).
23. Kizel' V.A., Burkov V.I. *Girotropiya kristallov* (Gyrotropy of Crystals) (Moscow: Nauka, 1980).
24. Rinkevichus V.S. *Lazernaya anemometriya* (Laser Anemometry) (Moscow: Energiya, 1978).
25. Klochkov V.P., Kozlov L.F., Potykevich I.V., Soskin M.S. *Lazernaya anemometriya, distantsionnaya spektroskopiya i interferometriya. Spravochnik* (Handbook of Laser Anemometry, Distance Spectroscopy and Interferometry) (Kiev: Naukova Dumka, 1985).